Transition modelling for viscous flow prediction

M.T. Arthur* and C.J. Atkin†
QinetiQ Ltd., Farnborough, Hampshire, GU14 0LX, UK

The paper describes a method for the calculation of viscous flows that includes the prediction of the transition onset location. It is an engineering approach aimed at providing a useful and necessary tool for air vehicle design and assessment. Some background that led to the adoption of the present approach is first given and the method is then described. Particular problems associated with the approach are identified and solutions are provided. Results from the initial validation of the method for both two- and three-dimensional flows are presented. The results illustrate the effects on flow-field predictions of modelling transition and the need to incorporate transition modelling in CFD methods is clearly demonstrated. The results also illustrate that the improved modelling can lead to a better understanding of the complex flows associated with some recent air vehicle designs, and the sensitivity of those flows to transition.

Nomenclature

C_p = pressure coefficient
M_∞ = free-stream Mach number
Re = Reynolds number
α = angle of incidence
η = non-dimensional spanwise coordinate

I. Introduction

UNDERSTANDING the process by which a laminar flow becomes turbulent provides perhaps the greatest technical challenge in aerodynamics. The transition process is complex and can occur through a number of mechanisms depending on the development of the boundary layer, on scaling parameters such as Reynolds and Mach numbers, on complex environmental factors (e.g. noise and free-stream turbulence) and on the properties of the surface (e.g. curvature and surface finish). A wide range of mathematical techniques has been brought to bear on the various different mechanisms involved but the complexity of some, and their extreme requirements in computing time, make them unsuitable for coupling to a CFD code for routine use. The modelling of transition for CFD is necessarily a compromise between fidelity and efficiency, much as with turbulence modelling. However, whereas with turbulence modelling researchers sought for many years for a universal model of turbulence before accepting that no such model existed, it is already known that there are several competing transition mechanisms (such as Tollmien-Schlichting waves, stationary cross-flow vortices, attachment line contamination and other so-called 'bypass' mechanisms) and so fundamentally different models of transition are required for transition prediction within a CFD code.

A. Empirical criteria

Much early work in transition modelling was devoted to identifying a point at which laminar flow became unstable, assuming that this was equivalent to the breakdown to turbulence. Initially it was assumed that this transition 'point' would correlate with some local flow property and a number of empirical transition criteria were developed by extensive experimentation and analysis. Despite the simplicity of the approach many of these criteria tried to include the observed sensitivity of transition to disturbances in the free stream and/or to surface finish. Though instability and transition are now known not to be coincident, empirical criteria of increasing complexity continue to be used for engineering purposes. Modern techniques correlate transition onset with one or more

* Principal Scientist, Aerodynamics and Aeromechanical Systems Department
† Principal Engineer, Aerodynamics and Aeromechanical Systems Department
.

functions of the developing mean flow and boundary layer (usually involving only integral properties such as displacement or momentum thickness, or shape factor). They are usually derived from correlations with experimental data although recently some have been refined using the results of linear stability analysis.

The nature of the derivation of the empirical techniques means that they are formally valid only for the range of flow types and parameter values over which the correlations have been performed. These constraints are rather difficult to quantify and so, therefore, is the validity of most empirical methods. In general they will give good indications of the response of transition to incremental changes in flow parameters only within these constraints. A good example is the failure of many Tollmien-Schlichting instability criteria (usually developed from incompressible flow correlations) to predict transition for compressible flows. For flow control applications, the development potential of empirical methods diminishes with the appearance of each new influence on the transition process, since the correlation exercise then becomes multi-dimensional and rather cumbersome. Empirical methods are very efficient, however, since they involve mainly algebraic expressions and therefore take a negligible amount of computing time when compared with the solution of a system of differential equations.

B. Convective disturbances and stability analysis

An alternative approach to transition onset prediction is the direct analysis of the stability of the boundary layer. The mathematical problem is simplified in two ways. Strictly speaking laminar-turbulent transition is a *global* instability of the flow field but a global analysis would be computationally prohibitive for routine use within a CFD framework. Most important transition mechanisms in external aerodynamics are convective in nature and the elliptic characteristics of the instabilities can be neglected with good accuracy. Secondly the majority of the growth of instabilities in the boundary layer occurs at low amplitudes and can be modelled using linear analysis (i.e. the instability modes can be treated as independent). Non-linear secondary instabilities play an important role in transition but often display very rapid growth so that breakdown to turbulence follows shortly afterwards. Linear analysis therefore captures the spatially-dominant parts of the transition process. Most importantly, the linear stability approach can reproduce accurately the response of the instabilities to pressure gradient, sweep, Mach and Reynolds numbers and many forms of flow control which manipulate the boundary layer profiles.

The method for transition onset prediction developed at QinetiQ and used to obtain the results presented in this paper is based on such a linear stability analysis. It has been developed for the prediction of external aerodynamic flows within a Reynolds-averaged Navier-Stokes (RANS) framework. It differs from the approach recently presented by Langtry et al.[1,2] and Menter et al.[3] which is an advanced correlation-based model using two transport equations, one for intermittency and the second for the transition onset momentum thickness Reynolds number. By its very nature, the latter method relies on the availability of the correlation data. It differs also from approaches which use stability analysis of disturbance modes through manual intervention; the present method is fully automated.

The essence of linear stability analysis is that disturbances can be represented by a superposition of modes which are solutions of the linearised, unsteady Navier-Stokes equations. Thus a combination of temporal-spatial waves is superimposed on a steady, mean boundary layer flow, the latter usually calculated using a CFD method. The boundary layer streamlines are assumed to be parallel, so that the derivatives of the mean flow are neglected except in the direction normal to the wing surface. This leads to a loss of accuracy but an important simplification to the mathematics whereby a three-dimensional partial-differential stability problem – which describes the behaviour of the *global* instability – is broken into a series of local, one-dimensional ordinary differential equations (ODEs) each of which can be solved to yield the local spatial growth rate of the disturbance. These spatial growth rates can then be integrated with respect to streamwise distance, from some initial condition, to yield disturbance amplitudes. The approach has one major drawback when applied to three-dimensional flows where the boundary layer excites a two-dimensional spectrum of disturbances (in temporal frequency and spanwise periodicity). Both of these properties need to be defined before the local ODEs can be solved and the growth rates integrated. For a given global instability mode the temporal frequency of the disturbance is constant across the boundary layer but this is not true of the spanwise periodicity. Once the global mode is broken up into a series of local modes the physics which determines the development of spanwise periodicity through the boundary layer is lost. Linear stability methods for three-dimensional flows therefore require an added empirical relationship, usually termed the 'integration strategy', which defines how the spanwise periodicity of a given disturbance varies through the boundary layer from some initial value.

The analysis uses no information about how perturbations are introduced into the boundary layer (the receptivity process), except to assume that the receptivity physics introduces a broadband spectrum of disturbances which all have comparable amplitudes at the neutral stability point (more correctly, neutral points since these vary from mode to mode). Likewise the analysis provides no information about the effect of the appearance of secondary

instabilities. Classical linear analysis assumes linear behaviour from an arbitrary initial amplitude right up to breakdown. Thus the amplitude, A, of a disturbance mode at a point downstream of the neutral point is expressed relative to the amplitude, A_0, at the neutral point by writing $N = \ln(A/A_0)$ so that N is a measure of the growth from the neutral point and varies through the boundary layer for each disturbance. Each mode will have its own N-factor curve (e.g. N vs. x) but the focus is on those modes which, at some point in the boundary layer, are locally the most-amplified disturbance: the relevant N-factors are combined to yield the 'envelope' curve of maximum N-factors over the boundary layer. Thus the envelope indicates the maximum amplification of any of the modes at a given streamwise location or, more usefully, at a given Reynolds number based on that distance. Correlations in which calculated N-factors are compared with measured transition positions have shown that transition usually occurs when the envelope N-factor reaches some critical value which depends upon surface finish and free-stream turbulence and noise levels. More sophisticated approaches use different critical N-factors for crossflow and Tollmien-Schlichting instabilities. Methods based on this analysis are known as e^N methods and the e^N transition criterion was proposed independently by Van Ingen[4] and by Smith and Gamberoni[5] as an engineering tool which combined all the unknowns (initial amplitude, non-linear behaviour) into one parameter, the critical N-factor at transition. Critical N-factors need to be obtained experimentally (for a given wind-tunnel or flight environment and surface manufacturing standard) by correlating N-factor calculations against transition measurements before the process can be applied in reverse for cases when transition is unknown. A critical N-factor criterion can be carried across from one boundary layer to another so long as the following do not change:

a. the receptivity processes;
b. the amplitudes between which the linear analysis was valid; and
c. the processes downstream of the 'linear' region.

The conditions will generally be satisfied during a series of tests in a given facility with a given model build standard. However they would not normally be satisfied across the range of real flows spanning evaluation and application (e.g. between tunnel and flight), and therefore the e^N criterion has met with mixed success.

The existence of instability waves in boundary layers is well documented and seems to be the most likely route to transition in a low disturbance environment. It is assumed by most current stability analysis tools that cross-flow and Tollmien-Schlichting instabilities dominate the natural transition process, though other mechanisms cannot be ruled out and this assumption may be a source of error. An important additional source of error in classical e^N methods is that they ignore curvature effects. It is known that curvature can have a significant affect on the stability of cross-flow modes in particular. The correct treatment of curvature is one of the principal drivers for the use of non-local linear methods.

C. More rapid techniques

An extension of linear stability analysis methods has been developed for rapid prediction of transition loci. It relies on the fact that the solution of the linear stability equations must be analytical functions of the local velocity profiles. Thus by compiling a simple database of the stability properties of model velocity profiles the engineer can reproduce the results of a linear stability analysis using a simple combination of data retrieval and algebraic processing. The validity of such methods is limited by the range of model profiles with which the particular method is equipped and by the reliability of the database system.

D. More accurate techniques

Linear stability analysis and the parallel flow assumption has been enhanced by the development of both non-parallel linear methods and weakly non-linear methods. The former take account of the slight divergence of the streamlines in a real laminar boundary layer. The latter solve the parabolized stability equations[6] and provide a useful means for gaining an improved understanding of complex transition phenomena such as cross-flow vortex saturation[7] and resonance between Tollmien-Schlichting modes. However, the methods are too computationally demanding for routine use in the engineering environment. The results presented in this paper were not obtained using any of these latter methods but through direct linear stability analysis only.

E. Implementation issues

The implementation of transition modelling within a CFD method is not straightforward. All models of the types described above require information about the boundary layer flow to a degree of accuracy that is higher than that required for conventional assessment or design with fixed transition. Furthermore, most models require a post-processing phase in which a most-amplified or critical instability is retrospectively selected as the transition mechanism. This suggests that any attempt to develop a transition model that operated in the same way as a

stochastic turbulence model would need to identify the range of possible disturbances in advance of the CFD analysis: this is an impossible task. An appropriate approach is via an active boundary condition in which transition modelling is used intermittently to adjust the boundary conditions supplied to the RANS solver. At the same time, earlier work at QinetiQ[8] and elsewhere[9] suggests that most CFD methods would require unrealistically high, normal-to-wall, mesh densities to yield boundary layer data of the level of accuracy required, even for a transition model based on simple empirical criteria. The approach adopted in the work presented here, therefore, is to use a specialised boundary layer solver to recalculate the laminar boundary layers from the surface pressure distribution obtained from the CFD method to provide the boundary layer properties required by the transition model. The latter is used to determine a new transition locus which is passed back to the CFD method to continue the calculation. The process is repeated periodically until the flow solution and predictions of transition loci have converged.

II. Description of Method

The tools used to determine the locus of transition from the CFD solution are the QinetiQ codes BL2D[10] and CoDS[11]. BL2D is a finite-difference Newton method for swept-tapered laminar boundary layers employing a fourth-order-accurate compact-difference scheme in the wall-normal direction. CoDS is a robust e^N method solving for the eigenvalues of Mack's stability equations[12] for three-dimensional parallel-flow boundary layers, also employing a fourth-order-accurate compact-difference scheme. Both methods are quasi-two-dimensional and are therefore applied to line-of-flight 'strips' distributed over the aerodynamic surfaces. Both methods have been extensively validated against other European codes during a succession of EU-funded laminar flow projects. For highly three-dimensional boundary layers the methods will omit a good deal of the flow physics of three-dimensional mean flow development and instability wave propagation: more advanced three-dimensional methods have already been developed but these have not yet been exhaustively tested for the purposes of CFD-coupled transition prediction. Since there are significant process issues with modelling natural transition in CFD, it seems appropriate to start work with the more robust transition-prediction toolset rather than the more accurate methods.

The principal input to CoDS is a set of three-dimensional boundary layer velocity profiles distributed over the wing chord for a given line-of-flight 'strip'. The stability of each profile is analyzed in isolation. A range of 'integration' schemes to determine N-factors from the large numbers of calculated eigenvalues is available; otherwise the method uniquely requires no further user input to analyze the stability of the boundary layer. CoDS initially locates a series of unstable modes in the mid-chord region of the boundary layer and then marches both downstream and upstream to locate the position of the neutral stability curve. Temporal and spatial frequency ranges are determined automatically to yield a set of N-factor curves which span all typical crossflow, oblique and Tollmien-Schlichting modes in the boundary layer. The underlying eigenvalue solver is of the 'shooting' type but a series of empirical checks has been devised and the occurrence of a 'false root' to the stability equations (not uncommon with many shooting methods) was last observed in 1997: this represents an eigenvalue failure rate of less than 1 in 10^8. CoDS therefore performs extremely well as a 'black-box' method, a key feature of any part of the CFD process.

As discussed earlier, ensuring that the laminar profiles obtained from RANS solvers are of sufficient accuracy for stability analysis can be expensive in terms of mesh requirements. Despite the limitations of boundary layer methods for topologically-complex flowfields, such methods provide a cheap alternative to laminar Navier-Stokes for those external aerodynamic components for which transition modelling is of interest. The BL2D code is therefore used to calculate the laminar velocity profiles which are to be analyzed for stability. BL2D is a first-order boundary layer method, currently operating exclusively in direct mode, and thus requires as input the development of the velocity field at the 'edge' of the boundary layer. In a viscous-coupled analysis the inviscid solution at the surface can yield the required velocity field but a RANS flowfield must either be interrogated to determine the boundary layer 'edge' or, as in the present case, the principal assumption of first-order boundary layer theory is invoked and the surface pressures are used to determine the total velocity at the boundary layer edge. The flow vector remains to be determined and, at present, a swept-tapered flow assumption is used to extract this using the sweep angles, line-of-flight geometry and total velocity distributions along each analysis strip. This approach is not ideal for low aspect-ratio components but remains in place for the time being.

The overall process works as follows. The viscous flow over the configuration of interest is first calculated with an initial guess at the transition onset location which should, ideally, be downstream of the converged, predicted value. A series of line-of-flight pressure distributions is extracted from the RANS solution at different positions across the span. These are separated into upper and lower surface flows (i.e. they are separated at the attachment line) and are passed to the laminar boundary layer prediction code to enable the boundary layers to be computed with greater fidelity, as described above, to allow a stability analysis to be performed. The stability analysis, together

with some kind of critical N-factor criterion, yields transition onset locations which are passed back to the RANS solver for further iterations. The process is said to have converged when the residuals are small and the surface pressures and predicted transition locations are not changing significantly. Previous work has shown that for some flows, for example where a high pressure gradient is sufficient to induce transition, it is important to check that the predicted transition loci are upstream of the initial guesses since otherwise reliance cannot be placed on the result; for such flows, a predicted transition onset location can more easily move upstream than downstream during the iterative process. An under-relaxation scheme is employed during the iterative process to reduce the risk of the predicted transition locus moving upstream of what should be its converged location.

Surface pressure distributions computed with RANS methods have been found to have oscillations in the neighbourhood of the attachment line. Furthermore, the peak computed pressure, indicating the proximity of attachment, may exceed the stagnation pressure (in two-dimensions) or be inconsistent with the wing sweep (in three dimensions). The boundary layer method will usually fail while forming boundary conditions during the pre-processing stage. In most cases, this unphysical behaviour can be eliminated through application of a Schumann filter designed to operate on stretched grids but any scheme that is adopted must retain the essential physics. The problem is illustrated by the example of Fig. 1 which shows a typical distribution of pressure in the vicinity of the hook of a slat, calculated using a RANS method. Oscillations can clearly be seen, but they are not apparent at the scale of conventional plots of pressure distributions. In addition, it is clear that a smoothing procedure might result in a significant change in the predicted location of maximum pressure, indicating an attachment position that is incompatible with the velocity vectors.

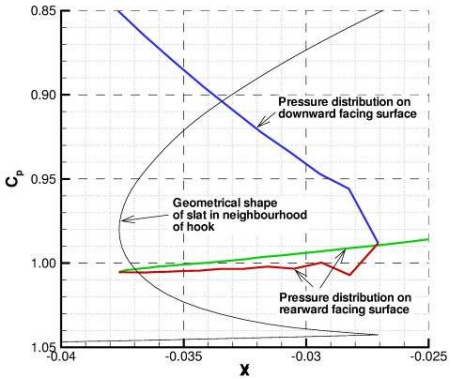

Figure 1. Typical computed pressure distribution in vicinity of hook of slat

A simple scheme has been devised which is robust but which, at the same time, preserves as much as possible of the true physics of the original solution. At each line-of-flight section of the wing at which the transition locus is defined, the location of attachment is calculated from the predicted surface pressure distribution. In general it lies between grid points and so the surface co-ordinates and value of attachment pressure coefficient are inserted into the data. The pressure distribution is then checked for oscillations in the vicinity of attachment and a Schumann filter is applied to remove them. The filter is applied in such a way that the peak pressure (i.e. the pressure at attachment) and its location are left unaltered by the filtering process. Next, the value of maximum pressure is compared to the stagnation pressure (for two-dimensional flows) or the theoretical attachment line pressure (for the given sweep angle for three-dimensional flows). If the predicted value exceeds the theoretical value, a further step is performed to reduce the peak pressure to an acceptable value.

III. Results and Discussion

The results presented here have been obtained using either the BAE SYSTEMS/Airbus multiblock code RANSMB or the irregular grid code, Jupiter, which is part of the Solar grid generation and flow solution system developed in the UK jointly by Airbus, BAE SYSTEMS, DERA and the Aircraft Research Association. RANSMB has been validated extensively for both military and civil configurations and its accuracy is similar to that of other good aeronautical CFD codes. Jupiter was developed more recently but is more versatile in terms of geometries for which suitable grids can be generated efficiently. It allows a wide range of options, for example in the choice of turbulence models, and not all of these have been validated to the same extent. However, it is widely used in the UK and performs well for a wide range of applications. Both codes were coupled to the transition onset prediction scheme described above for flow prediction with natural transition.

A. Guiding Principles

It was stated above that it was generally beneficial to begin a calculation with transition onset loci downstream of their final, predicted positions. This is partly because of the need to remove turbulence from a flow if a transition locus moves downstream, but mainly because of the influence of transition on the predicted development of the flow. This is very clear from Fig. 2 which shows the predicted pressure distribution over the CAST10 aerofoil obtained using three different approaches. The first had the initial transition location set at x/c=0.24 on the upper surface and x/c=0.496 on the lower surface; the relaxation factor was set at 0.5 initially but increased to 1 after the

predicted location of transition remained constant for three successive iterations. The second had the initial transition location set at x/c=0.55 on both surfaces and a relaxation factor set at 0.5 initially but increased to 1 when the predicted transition location moved downstream. The final calculation had the initial transition location set at x/c=0.9 on both surfaces and used a relaxation factor of 1. All the solutions are well converged.

Transition on the upper surface in the second calculation (relaxation scheme 2) resulted from laminar separation indicated by the boundary layer code and occurred at 38% chord. This is close to the value observed experimentally. However, the weak shock wave is not observed experimentally though similar features can be seen in solutions computed by other authors[9]. The location of transition on the lower surface from this calculation also resulted from laminar separation indicated by the boundary layer code and occurred at 52.1% chord.

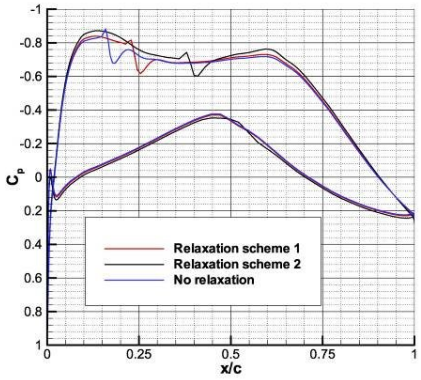

Figure 2. Predicted pressure distribution over the CAST10 aerofoil. $M_\infty = 0.725$, $\alpha = -0.35^o$, $Re = 3.9 \times 10^6$.

A flow feature such as a high pressure gradient may be associated with the onset of transition. A prediction of transition onset upstream of its true location, perhaps in the early stages of the iterative procedure when the flow solution is far from converged, may encourage the formation of such a feature which will, in turn, trigger transition in subsequent iterations of the coupling scheme. This will prevent the predicted location of transition onset from moving downstream towards its true position. Since the degree of upstream influence and whether or not features which may trigger transition will appear in the flow cannot be known in advance, the most reliable procedure appears to be to use an under-relaxation scheme and for the initial location of transition onset used by the RANS solver to be well downstream. At the same time, if the initial location of transition onset is too far downstream, it may destabilise the solver. As a general rule, under-relaxation of the predicted change in the location of transition onset at each iteration is sometimes necessary and never detrimental to obtaining an accurate solution.

B. High-lift Wing Section

The lift and drag coefficient curves for a two-dimensional, three-element, civil high-lift configuration are shown for several calculations and experiment in Fig. 3. The first and second sets of predictions were obtained using the multiblock code RANSMB with specified (i.e. fixed) transition loci. The second set of results was obtained some years ago using the k-g turbulence model. However, in later work at QinetiQ, Hutton, Ashworth and Peshkin[10] improved the implementation of the turbulence model and the first set of results was obtained using their variant of the code. Although there are significant differences in the results, it can be noted that both predict maximum lift at an angle of incidence approximately 2^o below that observed experimentally. Similarly, the rapid rise in predicted drag occurs at a much lower incidence than observed experimentally. It proved impossible to obtain converged solutions with either variant of the code at the next higher angle of incidence for which experimental data were available. The final set of results was obtained using the same computational grid and the Jupiter flow solver with natural transition. It can be seen that maximum lift is predicted to occur at approximately the same angle of incidence as in the experiment and that the drag rise is in much better agreement with experiment. Finally, it should be noted that the predicted coefficients were obtained by integration of pressure and skin friction coefficients at the nodes of the computational mesh, far greater in number than the points at which pressures were measured in the experiment. It was demonstrated in Garteur Aerodynamics Action Group AG25 that if the computed pressure coefficients were interpolated to the experimental stations and then integrated over that smaller number of points, much better overall agreement between prediction and experiment would be obtained. The effect on the distribution of surface pressure coefficient of

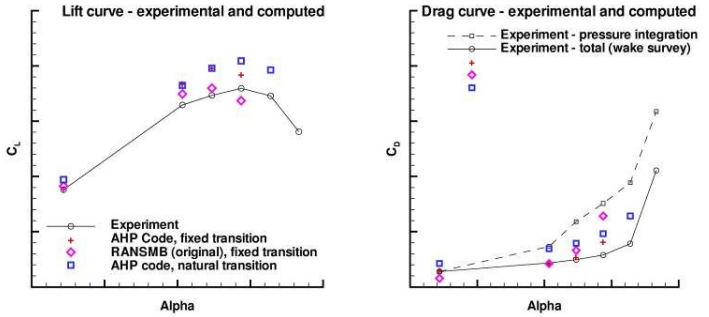

Figure 3. Lift and drag curves for a three-element, high-lift wing section. $M_\infty = 0.22$, $Re = 4 \times 10^6$.

including the prediction of transition onset location compared with the fixed transition locations used in earlier work is shown in Fig.4 for a typical case.

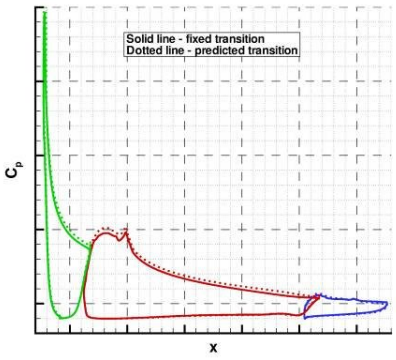

Figure 4. Predicted distribution of pressure coefficient over a three-element, high-lift wing section. $M_\infty = 0.22$, $Re = 4 \times 10^6$.

C. Civil Transport Wing

An important role that transition modelling can play in flow prediction is illustrated in Fig. 5. The case is a simple civil transport wing in transonic flow. The results were again obtained using the multiblock code RANSMB with the k-g turbulence model. The flow is relatively benign and so no under-relaxation was used when updating the transition loci from the predicted values. The figures show results from two sets of calculations. In the first set of results, the initial transition loci and the predicted loci at each iteration are shown. The leading and trailing edge positions of the wing are also indicated. It can be seen that, in all cases, the calculation of the transition locus converges very rapidly. The second set of results was obtained by setting the initial guess at the transition loci well forward on the wing. The final (i.e. converged) positions of the transition loci are shown and they are approximately coincident with the final values from the first set of calculations. This confirms the validity of the decision not to use under-relaxation in these case. Figures 5(a) and (b) show results for a Reynolds number 8.1×10^6 for the lower and upper surfaces respectively; it can be seen that there is a significant region of laminar flow on both surfaces and an apparently strong association between transition onset and the crank in the trailing edge. Compared with predictions obtained with transition fixed at 15% local chord on the upper surface and 5% local chord on the lower surface (which were the positions at which transition was fixed in wind-tunnel tests), there is an increase in lift of about 4.5% with natural transition. There is therefore an increase in induced drag but this is offset by reduction in friction drag from the larger region of laminar flow. In contrast, Fig. 5(c) shows results for the much higher Reynolds number 32.5×10^6 at which there is almost no laminar flow over the wing. This illustrates the dangers inherent in extrapolating from wind-tunnel results to full scale or, perhaps, the importance of correct and effective transition fixing for tunnel testing. At the same time, the results show the role that CFD can play in intelligent extrapolation or in reconciling observed differences between wind-tunnel and flight test results. The final skin friction predictions for the lower Reynolds number are shown for the central part of the wing in Fig.6.

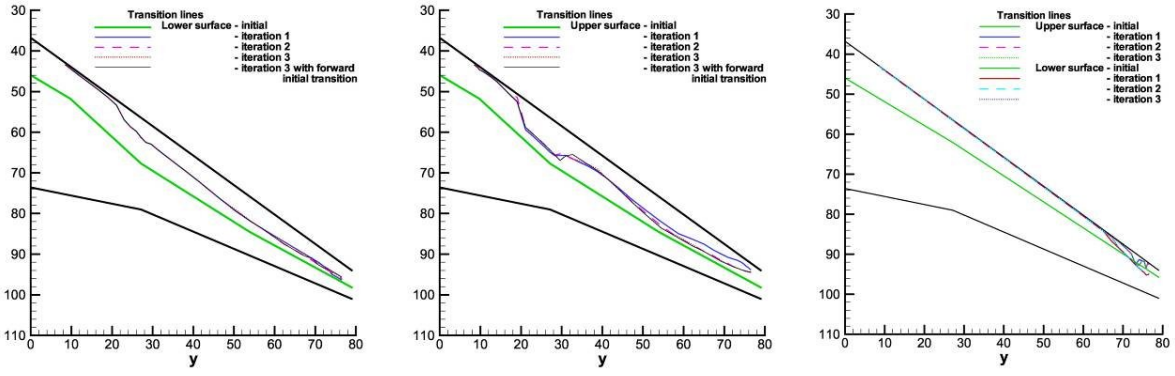

(a) **(b)** **(c)**

Figure 5. Sequence of transition loci predicted during the calculation of transonic flow over a civil transport wing. $M_\infty = 0.85$, $C_L \approx 0.5$: (a) and (b) $Re = 8.1 \times 10^6$; (c) $Re = 32.5 \times 10^6$.

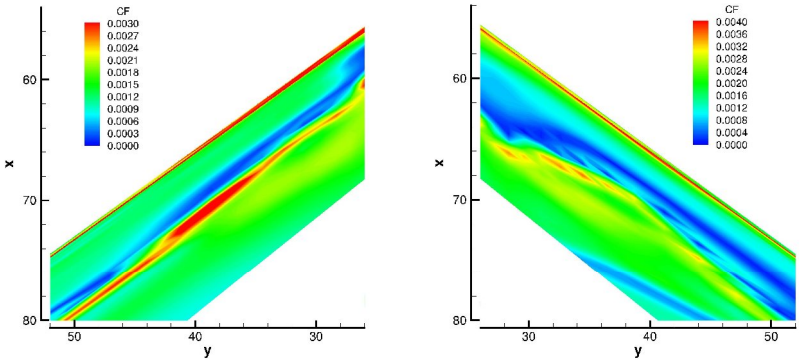

Lower surface **Upper surface**

Figure 6. Predicted variation of skin friction over the central part of the surface of a civil transport wing. $M_\infty = 0.85$, $C_L \approx 0.5$, $Re = 8.1 \times 10^6$.

D. Lambda wing configuration

A more complex three-dimensional configuration is provided by the lambda wing model M2382 shown in Fig. 7. Flow solutions with natural transition have been obtained using both the RANSMB and Jupiter flow solvers and distributions of surface pressure coefficient obtained using RANSMB are also shown in Fig. 7. The case is of separated, transonic flow, $M_\infty = 0.72$, $\alpha = 8.81^o$, $Re = 5.43 \times 10^6$ and is interesting because transition occurs through different mechanisms on different parts of the wing (though this is not an uncommon feature of three-dimensional flows). Although the model has been tested extensively, measurements of the transition onset location have not been made at these conditions. It turned out that the converged prediction of the transition onset locus on the lower surface, shown in Fig. 7, was well downstream of the initial location but once again, in this relatively benign flow, this appeared to cause no difficulty. The location of the initial locus was downstream of the predicted locus on the upper surface everywhere except in the region of the trailing edge crank. There is a strong influence of the crank on the surface pressure distribution and thus on transition onset, as observed in the case of the civil transport wing, Fig. 5. The case provides a further example in which correct transition fixing for a wind-tunnel test is impracticable but for which the impact on friction drag, and perhaps other forces and moments, will be significant.

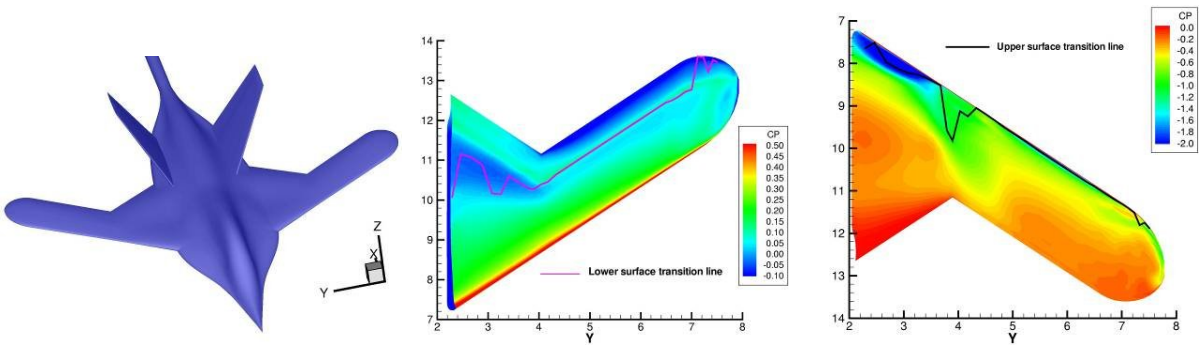

Figure 7. Lambda wing configuration

E. AFRL 1303 Unmanned Combat Air Vehicle concept

The AFRL 1303 unmanned combat air vehicle (UCAV) concept has been studied extensively in both experimental and computational programmes. In particular, an extensive programme of validation and evaluation has been undertaken by QinetiQ on behalf of the UK Ministry of Defence for a range of flow solvers and turbulence models against experimental data obtained in low-speed tests performed in the QinetiQ 5m wind tunnel at Farnborough[13, 14]. A selection of cases has been studied in a programme of work undertaken by The Technical Co-operation Programme (TTCP) under AER-TP5. Several variants of the 1303 model exist but the TTCP study has

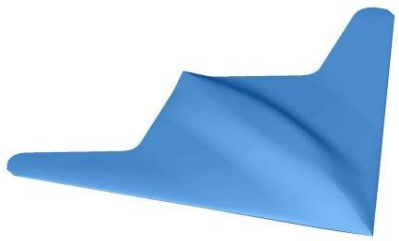

Figure 8. The computational model of the AFRL 1303 UCAV concept (sting not shown).

been concerned with a variant with a round leading edge known as the base-line leading edge. The programme of validation at QinetiQ has included the application of flow prediction with natural transition using the Jupiter flow solver as described in this paper.

Work presented elsewhere (see, for example, Ref. 14) shows that solutions of the RANS equations for the flow over the 1303 UCAV, especially in the important regime in which flow separation begins and develops, are sensitive to grid fineness, turbulence modelling and transition onset. The sensitivity to the grid relates especially to the fineness in the leading edge region where flow separation begins. Considerable care was therefore exercised in the generation of a set of grids for the study at QinetiQ. Further details are given in Ref. 14. The grids are block-structured and to facilitate the generation of good quality grid in the tip region, the computational model geometry was obtained from the wind-tunnel model by cutting off the tip at 98% semispan. The grid used to obtain the results presented here contains approximately 1 million cells and is the coarsest of the grids used in the QinetiQ study[14]. Care was also taken both in the initial choice and consistency of turbulence model parameters and boundary conditions. The k-g implementation[15] of Menter's turbulence model[16] is widely used in the UK aerospace industry and is the baseline model in the Jupiter flow solver. It was therefore adopted for the present calculations. However, work by Hutton[17] has shown that results obtained using the model are sensitive to the free-stream value of g and the first-order dissipation applied to k. Hutton demonstrated that satisfactory results could be obtained by setting g in the free stream to a value not far removed from that determined locally at the edge of the boundary layer and by switching off the first-order numerical dissipation on k. He suggested that the free-stream value of g should typically be in the range 0.3 to 0.8.

The results presented here were obtained with g set to 0.59 in the free stream. A suitable value of k was chosen by requiring the ratio of turbulent to laminar viscosity in the free stream to be 0.01. In cases for which the flow had separated, it proved impossible to obtain a sufficiently good flow solution with an initial transition locus anywhere on the upper surface. This is not surprising in view of the nature of the upper surface flow in the region of the leading edge. A fully turbulent flow was therefore obtained first for the results presented here. An initial transition onset locus was then determined from this in the manner described above (section II) and the calculation was continued to convergence in the usual way.

The 1303 computational model is shown in Fig. 8. A series of chordwise surface pressure distributions for the fully turbulent flow and flow with natural transition are compared with experimental data in Fig. 9 for flow conditions M_∞=0.25, α=7.60° and Re=4.3x10^6. It is important to note that the wind-tunnel tests were conducted to investigate the effects on the flow of varying both Mach and Reynolds numbers and that they were therefore carried out transition free. Over the inboard part of the wing, the effect of transition on surface pressures is small and the agreement both between the computations and with the experiment is good. By 70% semispan, however, the effects of separation can be seen in the fully turbulent flow prediction and there is a significant difference from the experimental result. The difference is significantly larger at 80% semispan. The prediction with natural transition recovers the difference and yields good agreement with experiment. At 90% semispan the experiment shows the flow to be separated but neither calculation exhibits the same characteristics. Grid refinement produces little improvement[14] and it may be that this difference in flow development is an effect of the difference in wing tip geometries of the computational and wind-tunnel models, as discussed above.

Figure 10 shows lines of skin friction on the upper surface of the configuration, with colour shading according to the pressure coefficient. A number of significant differences between the fully turbulent flow and flow with natural transition can be readily observed. A vortical separation develops in the fully turbulent flow (Fig. 10(a)) originating at about 60% semispan. The flow with natural transition clearly separates over the outer wing (Fig. 10(b)) but there is no indication in the pressure distribution (Fig. 9) of a vortex developing. The flow separation originates significantly further inboard in the flow with natural transition. This is compatible with a laminar separation and inspection of the results of the stability analysis confirms that a laminar separation is predicted outboard of approximately 23% semispan. Particularly interesting is the small feature close to the leading edge between 23% and 31% semispan. It is completely missing from the fully turbulent flow. A similar feature can be observed in oil flow photographs taken during the wind-tunnel tests[13] at the slightly lower Mach and Reynolds numbers, M_∞=0.17 and Re=2.0x10^6 respectively, at angles of incidence of both 6^o and 8^o, although care should be exercised in drawing a conclusion from such a comparison since it is known that the flow is sensitive to variations in Reynolds number[13].

The computed coefficient of skin friction on the upper and lower surfaces is shown for the same flow conditions for the fully turbulent flow in Fig. 11 and the flow with natural transition in Fig. 12. The differences for the

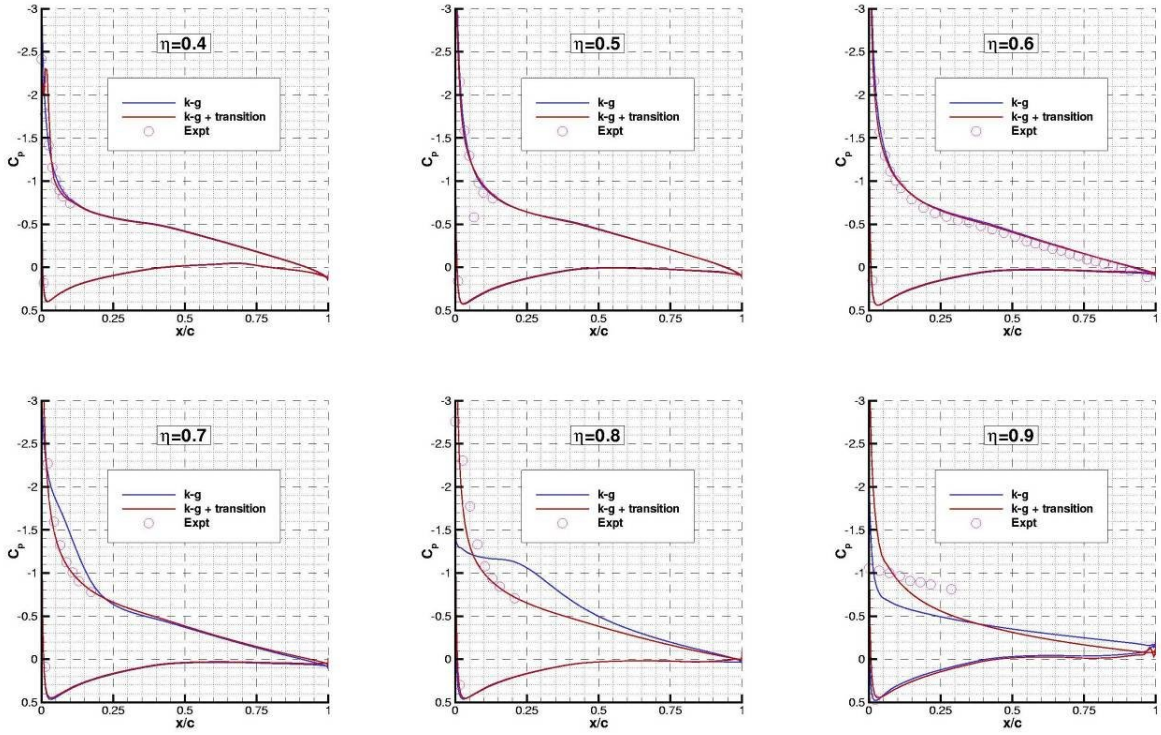

Figure 9. Comparison of experimental and computed pressure distributions for fully turbulent flow and flow with natural transition. M_∞=0.25, α=7.60°, Re=4.3x10^6.

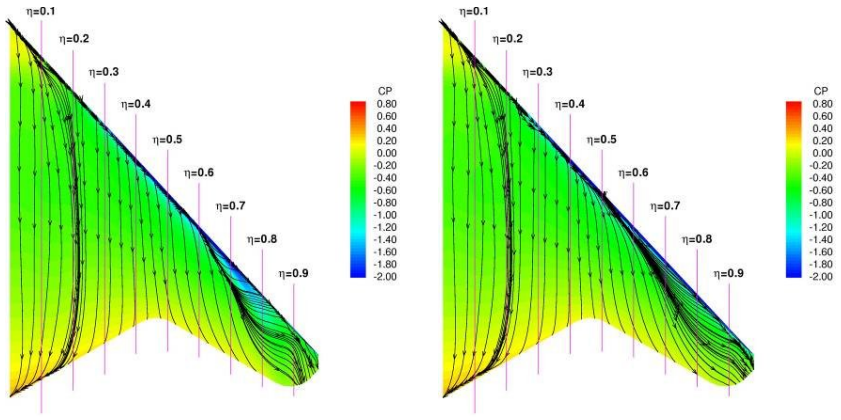

(a) **(b)**

Figure 10. Skin friction lines on upper surface of wing; surface coloured according to pressure coefficient. M_∞=0.25, α=7.60°, Re=4.3x10^6: (a) fully turbulent flow; (b) flow with natural transition.

upper surface are small, indicating that the flow is turbulent except close to attachment. There is a marked difference in the lower surface distributions, however, the flow with natural transition being laminar over much of the surface. This has a significant impact on the predicted drag coefficient, which is approximately 40 counts higher for the fully turbulent flow than for the flow with natural transition. Critical N-factors have not been measured for the 5m tunnel so that the latter drag figure, obtained using a $N = 9$ criterion, would be expected to under-estimate the experimentally measured drag.

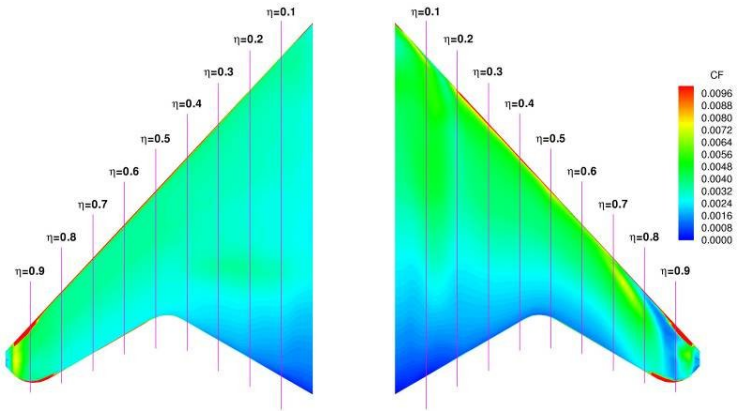

Lower surface **Upper surface**

Figure 11. Computed skin friction coefficient with fully turbulent flow. M_∞=0.25, α=7.60°, Re=4.3x10^6.

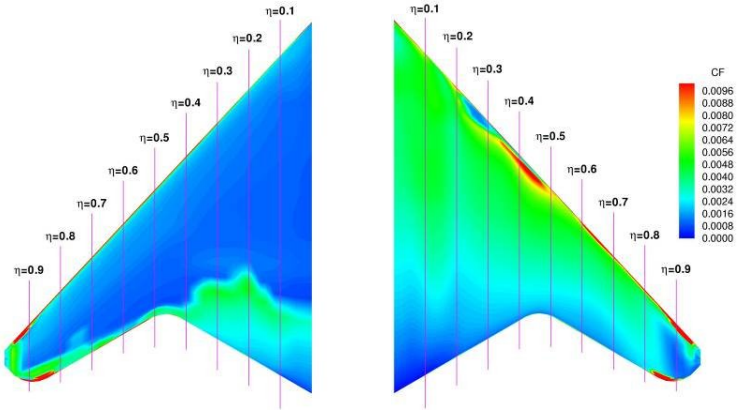

Lower surface **Upper surface**

Figure 12. Computed skin friction coefficient for flow with natural transition. M_∞=0.25, α=7.60°, Re=4.3x10^6.

IV. Conclusions

A method for calculating the external flow with natural transition over air vehicles has been developed and described. The method for transition onset prediction is based on the stability analysis of the laminar boundary layer and an e^N criterion to indicate transition. The stability analysis includes both Tollmien-Schlichting waves and cross-flow vortices. The method has been developed within a Reynolds-averaged Navier-Stokes framework and provides an automated method for the calculation of flow with natural transition.

The method has been applied to a range of two- and three-dimensional configurations and a selection of results has been presented here. The method has been shown to work and to be effective for a three-element aerofoil configuration and for three-dimensional configurations with a range of geometric and flow complexity. The results show the sensitivity of some flows to transition onset and thus Reynolds number. The dangers inherent in extrapolating experimental results and extending conclusions to conditions outside the range of Reynolds numbers tested is self-evident; however, the computational method presented here provides a means for performing that extrapolation to full scale and reduces the reliance on expensive, high Reynolds number test facilities. At the same time, the results demonstrate the need for correct and effective transition fixing in wind-tunnel experiments when that is appropriate.

The methodology employed is flexible and has enabled the transition prediction components to be coupled to different flow solvers with only minor revisions to the interfaces. Further work is required to extend the laminar

boundary layer calculation beyond separation, to incorporate the effects of attachment line contamination and receptivity, and also to include an intermittency model for the region over which transition from laminar to turbulent flow occurs. Some limitations of the present approach arising from the use of a swept-tapered boundary layer method were discussed in the paper and work on the development of a more advanced method is in hand. Additional work to improve the overall speed of flow prediction with natural transition is also underway. Nonetheless it is clear that the method provides a significant increment in the capability of the aerodynamic toolset used by those engaged in air vehicle design and assessment.

Acknowledgements

This work was undertaken jointly for the United Kingdom Ministry of Defence within the Weapons and Platform Effectors Domain under contract no. C/EGC/N03507, and for Airbus and DTI as part of the CAST 2 programme under project reference TP/2/5/ET/6/S/10264. The authors acknowledge the support of Dstl.

References

[1]Langtry, R.B. and Menter, F.R., "Transition modelling for general CFD applications in aeronautics", AIAA-2005-522, 43rd Aerospace Sciences Meeting & Exhibit, Reno, 2005.

[2]Langtry, R.B., Menter, F.R., Likki, S.R., Suzen, Y.B., Huang, P.G. and Völker, S., "A correlation based transition model using local variables Part 2 – Test cases and industrial applications", ASME-GT2004-53454, ASME TURBO EXPO 2004, Vienna, Austria.

[3]Menter, F.R., Langtry, R.B., Likki, S.R., Suzen, Y.B., Huang, P.G. and Völker, S., "A correlation based transition model using local variables Part 1 – Model formulation", ASME-GT2004-53452, ASME TURBO EXPO 2004, Vienna, Austria.

[4]Van Ingen, J.L., "A suggested semi-empirical method for the calculation of the boundary layer transition region", TU Delft Dept. Aero. Eng. report VTH-74, 1956.

[5]Smith, A.M.O. and Gamberoni, N., "Transition, pressure gradient and stability theory", Douglas Aircraft Co. report ES 26388, 1956.

[6]Herbert, T., "Parabolised stability equations", AGARD R 793.4, 1994.

[7]Atkin, C.J., Sunderland, R. and Mughal, M.S., "Parametric PSE studies on distributed roughness laminar flow control", AIAA-2006-3694, AIAA 3rd Flow Control Conference, San Francisco, CA, June 2006.

[8]Atkin, C.J., Algebraic transition modelling for flow control and simulation: final customer report, QINETIQ/FST/CR033413/1.0, November 2003.

[9]Houdeville, R., Arthur, M.T., Dol, H.S., Krumbein, A. and Ponsin, J., "Application of transition criteria in Navier-Stokes computations", GARTEUR TP-137, January 2003.

[10]Atkin C J. Calculation of laminar boundary layers on swept-tapered wings. QinetiQ unpublished technical report, February 2004.

[11]Atkin C J. User guide for CoDS version 3.3. DERA unpublished working paper, August 2001.

[12]Mack, L. M., "Boundary layer stability theory", AGARD Report 709, Chapter 3, 1984.

[13]McParlin, S.C., Bruce, R.J., Hepworth, A.G. and Rae, A.J., 'Low speed wind tunnel tests on the 1303 UCAV concept', AIAA-2006-2985, AIAA 24th Applied Aerodynamics Conference, San Francisco, CA, June 2006.

[14]Milne, M.E. and Arthur, M.T., "Evaluation of bespoke and commercial CFD methods for a UCAV configuration", AIAA-2006-2988, AIAA 24th Applied Aerodynamics Conference, San Francisco, CA, June 2006.

[15]Kalitzin, G., Gould, A.R.B. and Benton, J.J., "Application of two-equation turbulence models in aircraft design", AIAA 96-0327, 1996.

[16]Menter, F.R., "Two-equation eddy-viscosity turbulence models for engineering applications", AIAA Journal, Vol. 32, No. 8, 1994.

[17]Hutton, A.G., "Free-stream sensitivity of the k-g implementation of Menter's turbulence model", QINETIQ/FST/CAT/CR021146, February 2002.